Preliminary Analysis of Soil Retaining Walls for Railway Embankments Damaged by the 1995 Hyogoken-Nambu Earthquake

by

Junichi KOSEKI [1], Masaru TATEYAMA[2], Fumio TATSUOKA[3] and Katsumi HORII[4]

ABSTRACT

In order to improve current aseismic design procedures of retaining walls, external and internal seismic stability of different types of retaining walls for railway embankment, which were damaged by the Hyogoken-Nambu earthquake, was evaluated in the framework of the current design procedure based on the pseudo-static limit equilibrium method while neglecting the effect of vertical earthquake motion. The potential failure mode was compared with the actual behaviour, and the critical horizontal seismic coefficient which yields a safety factor of unity was compared with the estimated peak horizontal acceleration.

INTRODUCTION

The Hyogoken-Nambu Earthquake of January 17, 1995, caused serious damage to a number of conventional masonry and unreinforced concrete gravity-type retaining walls (RWs) for railway embankment. Many modern cantilever-type steel-reinforced concrete (RC) RWs were also damaged, while geogrid-reinforced soil retaining walls (GRS-RWs) having a full-height concrete facing performed very well during the earthquake (Tatsuoka et al., 1995 and Tatsuoka et al., 1996).

This paper will describe the results of back analyses by the pseudo-static limit equilibrium method on different types of five RWs at following four sites. These analyses were conducted to improve the current aseismic design procedures. **Fig. 1** indicates the locations of the sites and the areas where the Japanese seismic intensity scale was seven.

a) Sumiyoshi site (Leaning-type RWs along JR Tokaido Line between Setsu-Motoyama and Sumiyoshi Stations, **Fig. 2)**

Leaning-type unreinforced concrete RWs extending for a length of about 500 *m*, which were constructed 58 years ago (at the time of the earthquake), were broken and split off at the level of the ground surface, and the upper part overturned completely to the ground surface, resulting into the back face upside down. In some sections where the embedment depth was relatively small, the whole RWs overturned about the bottom.

b) Ishiyagawa site (Gravity-type RWs, **Fig. 3**, and cantilever-type RC RWs, **Fig. 4**, along Main Line of Hanshin Railway Co. adjacent to Ishiyagawa Station,)

Several sections of gravity-type unreinforced concrete RWs extending for a total length of about 400 *m*, which were constructed 66 years ago based on the standard design used at that time, tilted largely, while a 200 *m*-long section was broken at the construction joint at the mid-height level and overturned totally.

c) Shin-Nagata site (Cantilever-type RC RWs along JR Sanyo Line at Shin-Nagata Station, **Fig. 5)**

Cantilever-type RC RWs extending for a length of about 200 *m*, which were constructed 65 years ago possibly with a wooden pile foundation at the base of the RWs, suffered cracking at the mid-height level of the wall and the whole RWs largely tilted and slid outward at the bottom.

[1] Associate Professor, Institute of Industrial Science, University of Tokyo, Japan
[2] Chief Engineer, Railway Technical Research Institute, Japan
[3] Dept. of Civil Eng., University of Tokyo, Japan
[4] Director, System Development Div., Engineering Headquarters, Chuo Kaihatsu Corp., Japan

Cantilever-type RC RWs extending for a length of about 30 *m* tilted similarly to the adjoining gravity-type RW, while a section without counterforts suffered cracking at the mid-height level of the wall.

d) Tanata site (GRS-RWs along JR Tokaido Line between Ashiya and Setsu-Motoyama Stations, **Fig. 6**)

GRS-RWs having a full-height concrete facing extending for a length of about 300 *m*, which were completed in February 1992, deformed and moved slightly. The largest outward displacement was 26 *cm* and 10 *cm* at the top of the wall and at the ground surface level, respectively, at the highest part of the wall, adjacent to a RC box culvert crossing the railway embankment.

SURVEY OF SUBSOIL AND EMBANKMENT CONDITIONS

Results of borehole surveys on the subsoil conditions at the typical damaged cross-section of the RWs are shown in **Figs. 2 to 6**. The subsoils consist of, from the top, Holocene fan deposits (denoted as As and Ac in the figures), Later Pleistocene terrace deposits (Ts and Tg) and Middle Pleistocene terrace deposits (Os and Oc).

Fig. 7 shows the typical grain size distributions of the fill materials for embankment. **Table 1** summarizes their property evaluated by in-situ unit weight tests. The fill material at Shin-Nagata site was a relatively loose sandy soil containing a large amount of fines, while those at other sites were Masa-soils (decomposed granite soil), which were almost similar to each other. A series of CD triaxial compression tests on samples recompacted to the field density and water content. The confining pressures employed were relatively low, typically 9.8, 29.4, and 98 *kPa*, so as to simulate the field low pressure levels. The shear resistance angle ϕ_d was evaluated by assuming that the cohesion c_d is zero.

ESTIMATION OF PEAK GROUND ACCELERATION

Damage to wooden houses in the adjacent area of the four sites was investigated after the earthquake and was summarized in **Fig. 8**, where their collapse ratios at and near the sites were equal to or higher than 30 %. These values are consistent with the fact that all the sites were located in the most severely shaken area as shown in **Fig. 1**. In the following analyses, the peak horizontal acceleration a_{hmax} at the four sites was roughly estimated to be between 600 and 800 cm/sec^2, which is based on the distribution of peak ground acceleration estimated by Sato (1996) as shown in **Fig. 9**.

STABILITY ANALYSES BASED ON CURRENT DESIGN PROCEDURE

In the framework of the current design procedure as specified in Design Standard for Railway Retaining Wall Structures (Japan National Railway, 1986) and Design Standard for Railway Earth Structures (Railway Technical Research Institute, 1992), stability analyses by the pseudo-static limit equilibrium method were performed to evaluate the critical seismic coefficient yielding a safety factor of unity. In the analyses, the effect of vertical earthquake motion was not taken into account, but it can be implicitly reflected by selecting a proper value of correction factor, as will be mentioned later.

Analyses of external stability against sliding, overturning, and bearing capacity and those of internal stability with respect to shear, tensile and compressive failure of the concrete wall structures were conducted based on the design parameters summarized in **Tables 2 and 3**, respectively. The conditions of the embankment and the subsoil were determined based on the results of in-situ and laboratory tests, while that of the concrete walls was determined from the tests on cored samples.

In the analysis for overturning stability, the center of rotation was assumed to be at the toe of the wall structure. The bearing capacity q_u of the subsoil was estimated by the following equations;

$$q_u = \{I_\gamma \cdot \beta \cdot \gamma_1 \cdot B' \cdot N_\gamma + I_q \cdot \gamma_2 \cdot D_f \cdot (N_q - 1)\}/F_s + \gamma_2 \cdot D_f \quad (1)$$

$$B' = B - 2 \cdot e \quad (2)$$

$$I_\gamma = (1 - \delta_L/\phi)^2 \quad (3)$$

$$I_q = (1 - \delta_L/90)^2 \quad (4)$$

where N_γ and N_q are coefficients of bearing capacity shown in **Table 2**, which were calculated based on the shear resistance angle ϕ estimated by the current design procedure. γ_1 and γ_2 are submerged or wet unit weight of subsoil below and above the bottom of retaining wall, respectively. β is a shape factor which was assigned to be 0.5 considering the continuity of the wall in the longitudinal direction. D_f is a depth of embedment. B is a bottom width of retaining wall, and B' is an effective bottom width. e is an eccentricity of load measured from the center of the bottom of the wall. I_γ and I_q are factors to correct for the effects of inclined loads (if $\delta_L > \phi$, then $I_\gamma = 0$), and δ_L is a direction of the inclined load defined from the upward direction.

The earth pressure acting from the backfill soil was evaluated by the trial wedge method as schematically shown in **Fig. 10**, where the angle α of the slip surface measured from the horizontal direction was changed to obtain the maximum earth pressure. To avoid an unrealistically long wedge at a small angle of α, a vertical slip surface at a horizontal distance of 20 *m* from the actual or virtual back face of the wall, which was roughly assigned considering the general dimension of the embankment, was assumed as shown in **Fig. 10**. The earth pressure was assumed to distribute vertically similar to hydrostatic pressure.

By this way, the safety factor for each of the aforementioned failure modes for a given horizontal seismic coefficient k_h was calculated. By repeating this procedure, the relationship between safety factor and the horizontal seismic coefficient k_h was obtained for each case. Note that the effects of earthquake motion on the subsoil below the ground surface was not considered in evaluating the active and the passive earth pressure, while the inertial force F for the wall structure embedded below the ground surface was reduced by the following equation;

$$F = k_h \cdot (W - \gamma_2 \cdot V) \tag{5}$$

where W and V are weight and volume of the wall structure embedded below the ground surface, respectively, and γ_2 is the wet unit weight of subsoil above the bottom of retaining wall.

The relationships between the horizontal seismic coefficient k_h and the safety factor for external stability are shown in **Fig. 11**. The potential failure mode which yields the smallest seismic coefficient is that due to the lack of bearing capacity in the subsoil layer beneath the wall for the gravity-type RW at Ishiyagawa and the cantilever-type RC-RWs at Ishiyagawa and at Shin-Nagata, while it is overturning for the leaning-type RW at Sumiyoshi and the GRS-RW at Tanata. Note that the safety factor against bearing capacity is taken as zero when overturning failure is expected to occur. Therefore, for Sumiyoshi site, the zero safety factor for bearing capacity failure shown in **Fig. 11(a)** is only the result of the safety factor less than unity for overturning, and it has no indication for the potential bearing capacity failure. For the RWs at Sumiyoshi, Ishiyagawa and Tanata sites, the expected failure modes are consistent with the observed ones as far as external instability is concerned. It is to be noted, however, that at Shin-Nagata site, the safety factor against bearing capacity failure without seismic effect (i.e. $k_h = 0$) is already less than unity. This result is not realistic. This unrealistic result may be attributed to possible existence of wooden piles used to reinforce the subsoil underlying the wall, which are indicated in the original design sheets. Their contribution, however, was ignored in the stability analyses. During the restoration work after the earthquake, it was attempted to identify the piles by excavating the subsoil partly, but they were not found. In spite of this, their existence, which alters substantially the potential failure mode of the wall for external stability from bearing capacity to overturning and sliding, was assumed in the following analyses considering the fact that the wall had been actually stable before the earthquake.

From the above, the critical horizontal seismic coefficients which yield the safety factor of unity were evaluated as 0.38, 0.25, 0.56, 0.18 and 0.40 for the leaning-type RW at Sumiyoshi, the gravity-type RW and the cantilever-type RC RW at Ishiyagawa, the cantilever-type RC RW at Shin-Nagata and the GRS-RW at Tanata site, respectively.

In these external stability analyses, the possible link between the bearing capacity failure and the overturning failure was not considered. It is quite possible that the center of rotation moves inward from the toe of the wall by the yielding in the subsoil beneath the toe of the wall, which leads to the decrease in the safety factor against overturning failure. This factor is particularly important for a rigid wall structure having a relatively wide base, i.e., gravity-type and cantilever-type RC RWs. Therefore, in analyses taking

into account this factor, the safety factor against overturning failure for Ishiyagawa and Shin-Nagata sites will become lower than those shown in **Fig. 11**. This issue is beyond the scope of this paper and will be studied in the near future.

Fig. 12 shows the relationships between the horizontal seismic coefficient k_h and the safety factors for internal stability, where the safety factors were plotted on a logarithmic scale because they changed very largely with changes in the seismic coefficient. For the leaning-type RW at Sumiyoshi, the gravity-type RW at Ishiyagawa and the GRS-RW at Tanata site, the safety factor against tensile failure of wall structure (reinforcing steel bar for GRS-RW and unreinforced concrete for other RWs) was smallest, while the potential failure mode was shear failure for the cantilever-type RC RWs at Ishiyagawa and Shin-Nagata sites. The critical horizontal seismic coefficients which yield a safety factor of unity were 1.00, 0.32, 0.75, and 0.70 for Sumiyoshi, Ishiyagawa (gravity-type), Ishiyagawa (cantilever-type), and Shin-Nagata site, respectively. The critical coefficient for the gravity-type RW at Ishiyagawa site would be even smaller if the reduction of strength at the construction joint could be taken into account in the analyses.

It should be noted that the safety factor for internal stability at Tanata site was always larger than 1.0, which supports the fact that the facing of the GRS-RW was not damaged. This fact demonstrates that the facing with a minimal width of 30 to 55 *cm* was strong enough to survive the earthquake. This high safety factor, despite a relatively small facing thickness, is due to the fact that the facing behaves like a continuous beam supported by a number of points with a short span equal to a vertical spacing of reinforcement layers, 30 *cm*. This is in contrast with the fact that the other types of retaining walls behave like a cantilever beam supported only at the base.

CORRECTION FACTORS

Obviously, the use of the peak horizontal acceleration divided by g as the horizontal seismic coefficient in the pseudo-static limit equilibrium-based stability analysis is not appropriate, but the value corrected by being multiplied by a factor C less than unity should be used. The correction factor C can be defined as

$$C = k_{h,crit}/(a_{hmax,crit}/g) \tag{6}$$

where $a_{hmax,crit}$ is the critical peak horizontal acceleration which just triggers failure of the wall, and $k_{h,crit}$ is the equivalent critical horizontal seismic coefficient which yields safety factor of unity by the pseudo-static limit equilibrium-based stability analysis.

In this study, $k_{h,crit}$ for external and internal stability was evaluated for the five RWs at the four sites as mentioned in the preceding section excluding that at Tanata site for internal stability, while the estimated range of the peak horizontal acceleration a_{hmax}, which is between 600 and 800 cm/sec^2, was substituted into $a_{hmax,crit}$ in Eq. (6). This substitution will result in underestimation of C for RWs which actually failed because a_{hmax} should be larger than $a_{hmax,crit}$. On the other hand, the value of C is overestimated for a wall which did not fail but may fail for the peak ground acceleration larger than a_{hmax}.

Fig. 13 shows the values of C for external stability obtained from the analyses considering and not considering the effects of vertical acceleration. It may be seen that the values of C are between 0.2 and 0.6 except for the cantilever-type RC RW at Ishiyagawa site. A relatively large value for the cantilever RC RW at Ishiyagawa site may be consistent with the actual extent of failure that during the earthquake the wall was relatively stable compared with the other conventional type RWs. This value will, therefore, not be referred to below. Note, however, that the other conventional type RWs at Sumiyoshi, Ishiyagawa (gravity-type) and Shin-Nagata sites were seriously damaged and removed for reconstruction after the earthquake, while GRS-RW at Tanata site was only slightly damaged and has been reused at the slightly displaced position. This inconsistent result may have resulted from inconsistencies in the current design methods for these different types of RWs. Based on the actual damage and the need for reconstruction, the actual value of C to be adopted for external stability analysis in the framework of the current design standards, which do not consider the vertical earthquake motion, may be larger than 0.6 (but less than 1.0) for the leaning-type, gravity-type and cantilever-type RWs, while this value may be smaller than 0.6 for

GRS-RWs. Ductile behaviour of GRS-RW together with hidden conservatism in its current design procedure was discussed by Tatsuoka et al. (1996), but it is still a matter for further study.

The values of C for internal stability are indicated in **Fig. 14**. For the gravity-type RW at Ishiyagawa site, the correction factor is as low as about 0.5, which may be even lower if the strength reduction at the construction joint is taken into account. This low value of C is consistent with the fact that a section of the gravity-type wall was broken at the construction joint at the mid-height level as mentioned before. In contrast to this, the value is around 1.0 for the cantilever-type RC RWs at Ishiyagawa and Shin-Nagata sites. This value of C may be consistent with the overall occurrence of cracking in these cantilever-type RC RWs. This result indicates only that the correct value of C should be larger than unity. Furthermore, a correction factor between 1.2 and 1.6 evaluated for the leaning-type RW at Sumiyoshi site may reflect such a marginal situation as that breakage of the wall at the level of the ground surface partly occurred. Comparison of this value with the corresponding range for external stability shown in **Fig. 13** leads to a suggestion that the actual value of C to be used for internal stability analysis should be larger than that for external stability analysis.

CONCLUSIONS

A variety of retaining walls for railway embankment in areas shaken severely by the 1995 Hyogoken-Nambu earthquake performed differently. The potential failure mode expected from the results of pseudo-static limit equilibrium-based stability analyses based on the current design procedure while neglecting the effect of vertical earthquake motion were generally consistent with the observed behaviour.

The correction factor C was defined as the ratio of the critical horizontal seismic coefficient which yields a safety factor of unity to the coefficient corresponding to the estimated peak horizontal acceleration which triggers failure. It was estimated that for seriously damaged walls (leaning-type, gravity-type and cantilever-type RC RWs) a value of C larger than 0.6 (but perhaps less than 1.0) should be used to convert the design peak horizontal acceleration divided by g into the design seismic coefficient to be used in the pseudo-static limit equilibrium-based external stability analysis. On the contrary, it was suggested that for geogrid-reinforced soil RWs, a value of C equal to 0.6 for external stability is still conservative. Furthermore, it was suggested that the correction factor for internal stability may be even larger than these values for external stability.

Further investigation is required on the effect of vertical earthquake motion and on the difference in this factor for different types of RWs including the effects of the ductile behaviour of GRS-RW together with the hidden conservatism in its design procedure.

ACKNOWLEDGMENTS

The authors wish to thank Mr. S. Nishihara of Chuo Kaihatsu Corporation for his assistance in the preparation of this paper.

REFERENCES

1) Japan National Railway (1986): Design Standard for Railway Retaining Wall Structures (in Japanese).
2) Railway Technical Research Institute (1992): Design Standard for Railway Earth Structures (in Japanese).
3) Sato, T. (1996): Estimation of Maximum Ground Motion in the Area of Seismic Intensity 7, *Tsuchi-to-Kiso*, Vol.44, No.2, pp.35-37 (in Japanese).
4) Tatsuoka, F., Koseki, J., Tateyama, M. and Horii, K. (1995): Performance of Soil Retaining Walls during the Great Hanshin-Awaji Earthquake, *Bulletin of ERS, No.28,* pp.43-57.
5) Tatsuoka, F., Tateyama, M. and Koseki, J. (1996): Performance of Soil Retaining Walls for Railway Embankments, *A Special Issue of Soils and Foundations on Geotechnical Aspects of the January 17 1995 Hyogoken-Nambu Earthquake*, pp.311-324.

Table 1 Property of fill materials for embankment

Site	In-situ unit weight test				Triaxial tests (CD) of recompacted samples			
	G_s	γ_t kN/m³	w %	e	γ_t kN/m³	γ_d kN/m³	e	ϕ_d* degree
Sumiyoshi	2.630	18.04	6.7	0.525	18.04	16.91	0.525	45.8
Ishiyagawa	2.639	17.40	8.5	0.613	18.03	16.62	0.556	43.7
Shin-Nagata	2.662	16.09	10.4	0.790	15.91	14.41	0.811	35.3
Tanata	2.682	16.69	5.0	0.654	17.05	16.24	0.619	42.4

*Shear resistance angle was obtained by assuming that the cohesion c_d is zero.

Table 2 Design parameters for external stability analyses

Site		Sumiyoshi (Leaning type)	Ishiyagawa (Gravity type)	Ishiyagwa (Cantilever type)	Shin-Nagata (Cantilever type)	Tanata (GRS-RW)
Schematic diagram		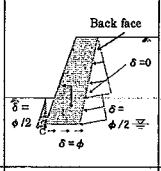	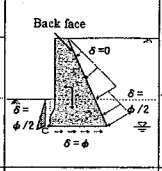	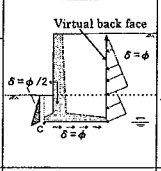	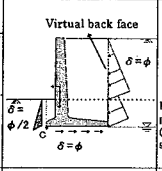	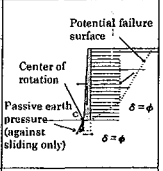
Concrete wall	γ (kN/m³)	0.241	0.235	0.233	0.241	0.255
Soil property used to evaluate earth pressure	γ (kN/m³)	0.188	0.181	0.181	0.167	0.173
	c (kN/m²)	0.0	0.0	0.0	0.0	0.0
	ϕ (°)	45	42	42	36	41
Soil property used to evaluate bearing capacity	γ (kN/m³)	0.205	0.197	0.197	0.179	0.180
	c (kN/m²)	0.0	0.0	0.0	0.0	0.0
	ϕ (°)	41.8	35.8	35.8	31.0	33.4
Coefficient of bearing capacity	N_γ	138	32.4	32.4	9.7	—
	N_q	79	24.0	24.0	9.8	—

Table 3 Design parameters for internal stability analyses

Site		Sumiyoshi (Leaning type)	Ishiyagawa (Gravity type)	Ishiyagawa (Cantilever type)	Shin-Nagata (Cantilever type)	Tanata (GRS-RW)
Schematic diagram		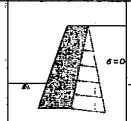	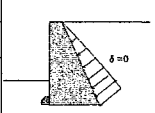	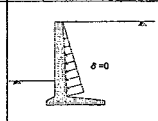	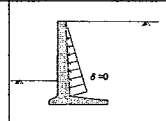	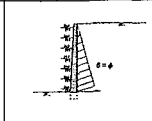
Concrete	γ (kN/m³)	0.241	0.235	0.233	0.241	0.255
	Compressive strength (kN/m²)	1.94	1.96	3.17	2.68	2.14
	Tensile strength (kN/m²)	0.172	0.147	—	—	—
Steel bar	Tensile strength (kN/m²)	—	—	24.5	30.6	30.6
	Cross-sectional Area (m²/m)	—	—	4.23×10^{-4}	19.4×10^{-4}	5.07×10^{-4}

Table 4 Potential failure modes and critical seismic coefficients for external and internal stability

Site	Type of RW	External stability		Internal stability	
		Failure mode	$k_{h,crit}$	Failure mode	$k_{h,crit}$
Sumiyoshi	Leaning	Overturning	0.38	Tensile failure	1.00
Ishyagawa	Gravity	Bearing capacity	0.25	Tensile failure	0.32
Ishiyagawa	Cantilever	Bearing capacity	0.56	Shear failure	0.75
Shin-Nagata	Cantilever	Sliding*	0.18*	Shear failure	0.70
Tanata	GRS	Overturning	0.40	—	—

*Potential failure mode was obtained by assuming an existence of wooden piles in the subsoil beneath the RW at Shin-Nagata site, where the safety factors were almost similar against both sliding and overturning.

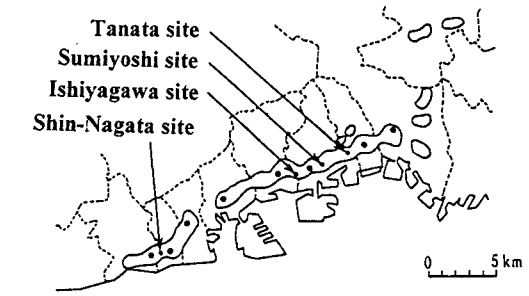

: Areas of Japanese seismic intensity scale of seven (According to Japan Meteorological Agency)

Fig. 1 Areas of Japanese seismic intensity scale of seven and locations of retaining walls (RWs) reported in this paper

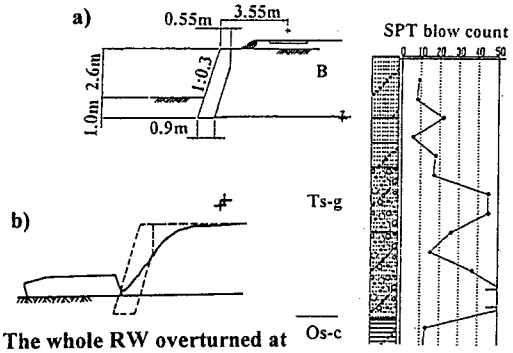

The whole RW overturned at some sections where the embedment depth was relatively small.

Fig. 2 Leaning-type RW at Sumiyoshi site; a) cross-section and b) sketch

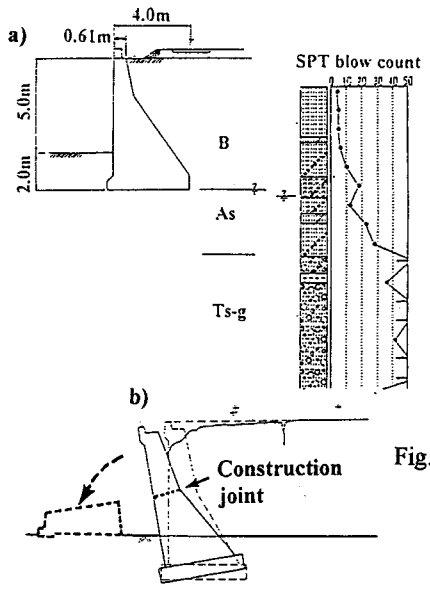

Fig. 3 Gravity-type RW at Ishiyagawa site; a) cross-section and b) sketch

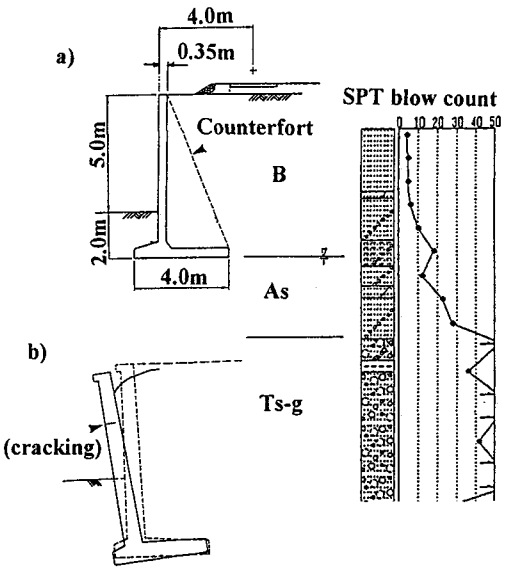

Cracking of the RC wall was observed at a section without counterforts.

Fig. 4 Cantilever-type RC RW at Ishiyagawa site; a) cross-section and b) sketch

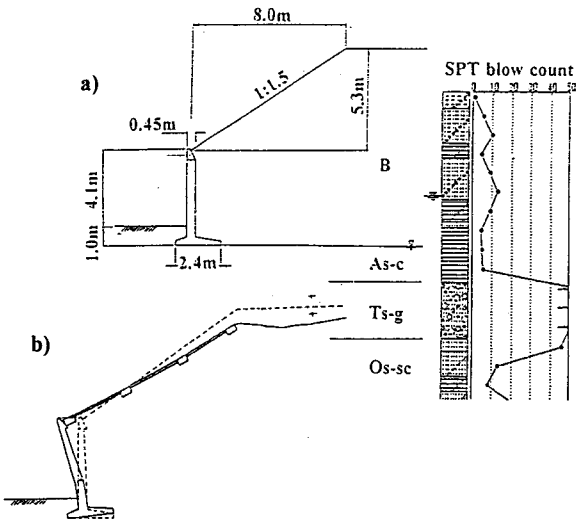

Fig. 5 Cantilever-type RC RW at Shin-Nagata site; a) cross-section and b) sketch

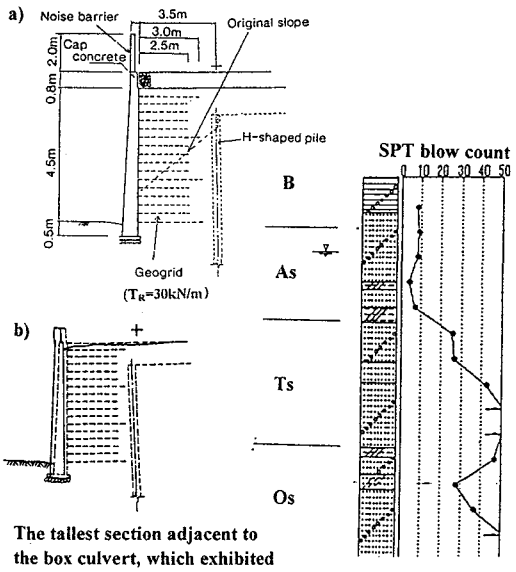

The tallest section adjacent to the box culvert, which exhibited the largest displacement, is shown.

Fig. 6 GRS-RW at Tanata site; a) cross-section and b) sketch

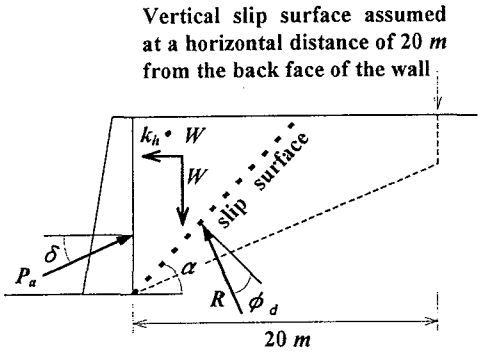

Fig. 10 Schematic diagram on trial wedge method

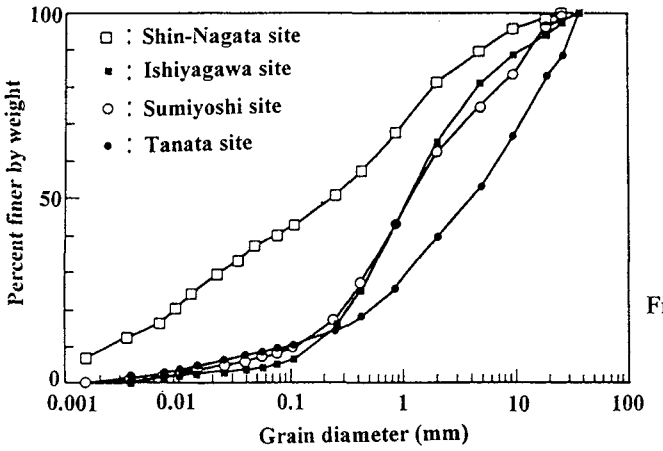

Fig. 7 Grain size distribution of the fill materials for embankment

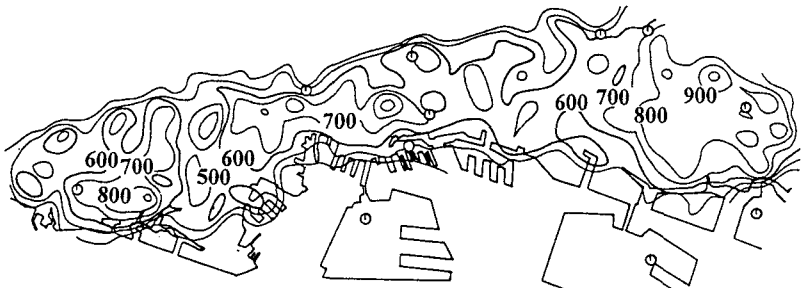

Number indicates the peak horizontal ground acceleration in cm/sec^2.
Ⓣ: Sites of strong motion observation

Fig. 9 Estimated distribution of peak horizontal acceleration (after Sato, 1996)

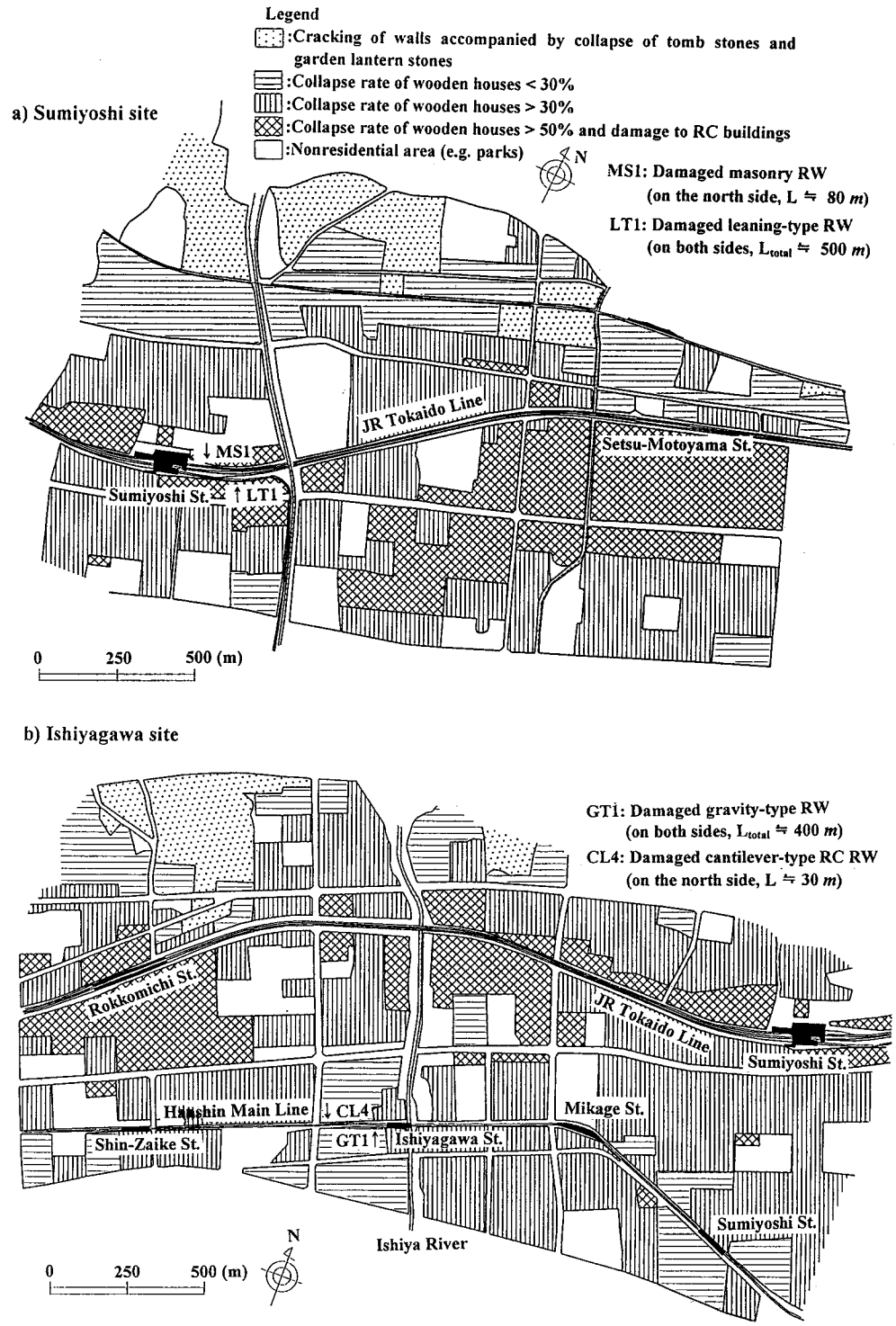

Fig. 8 Collapse ratio of wooden houses near the sites; a) Sumiyoshi site, b) Ishiyagawa site, c) Shin-Nagata site and d) Tanata site

c) Shin-Nagata site

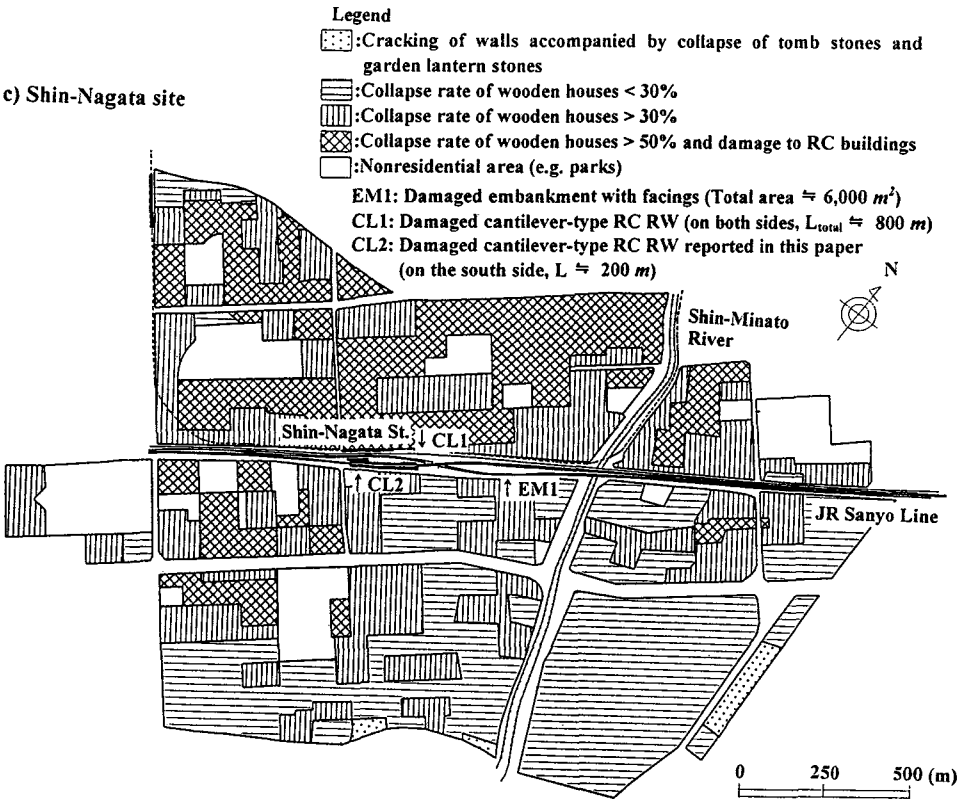

d) Tanata site

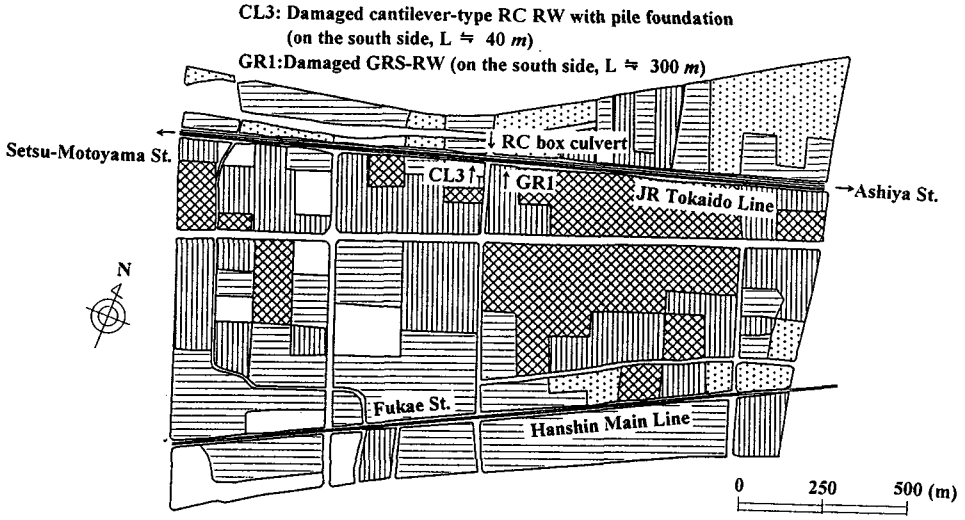

Fig. 8 (continued)

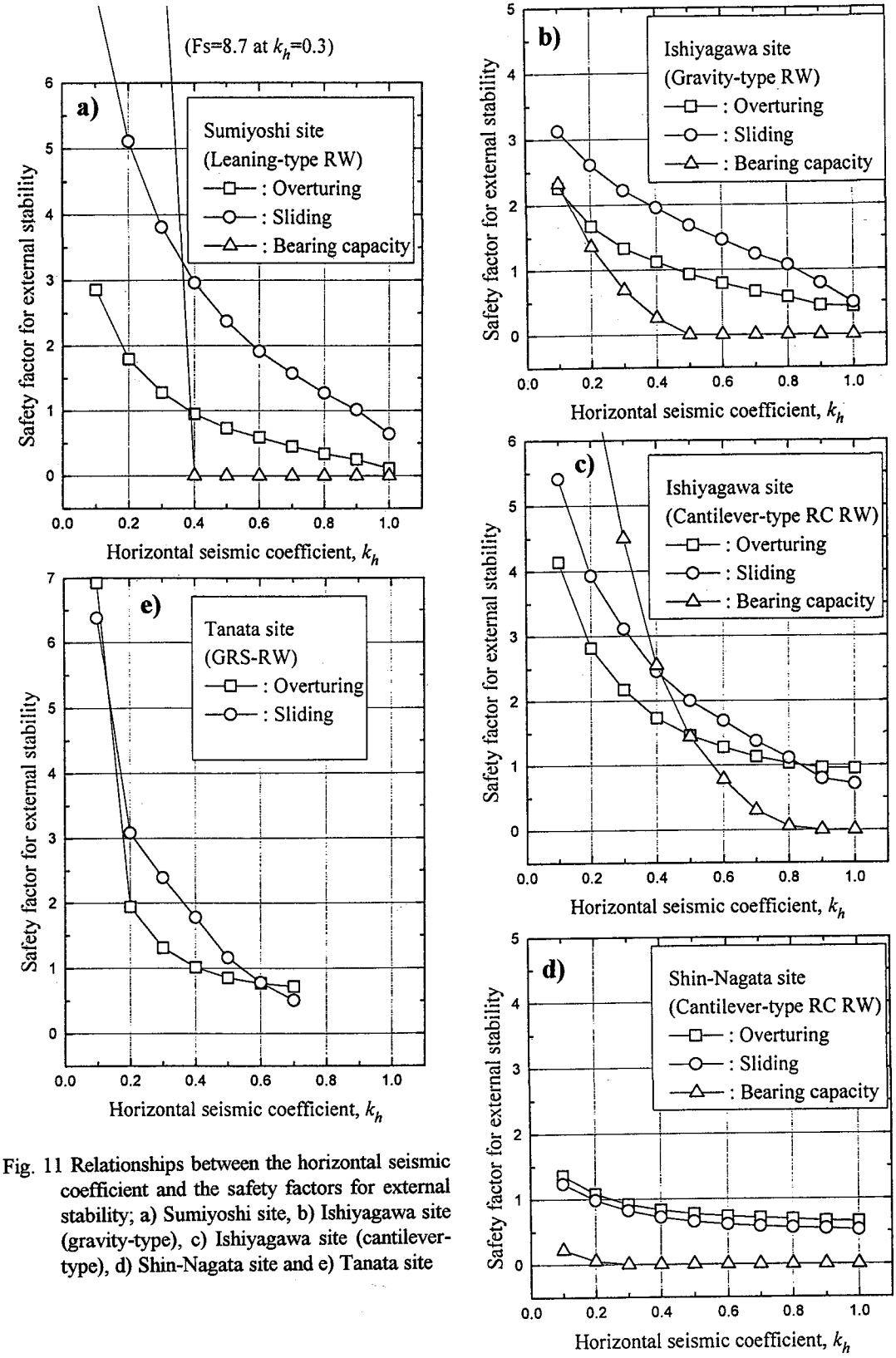

Fig. 11 Relationships between the horizontal seismic coefficient and the safety factors for external stability; a) Sumiyoshi site, b) Ishiyagawa site (gravity-type), c) Ishiyagawa site (cantilever-type), d) Shin-Nagata site and e) Tanata site

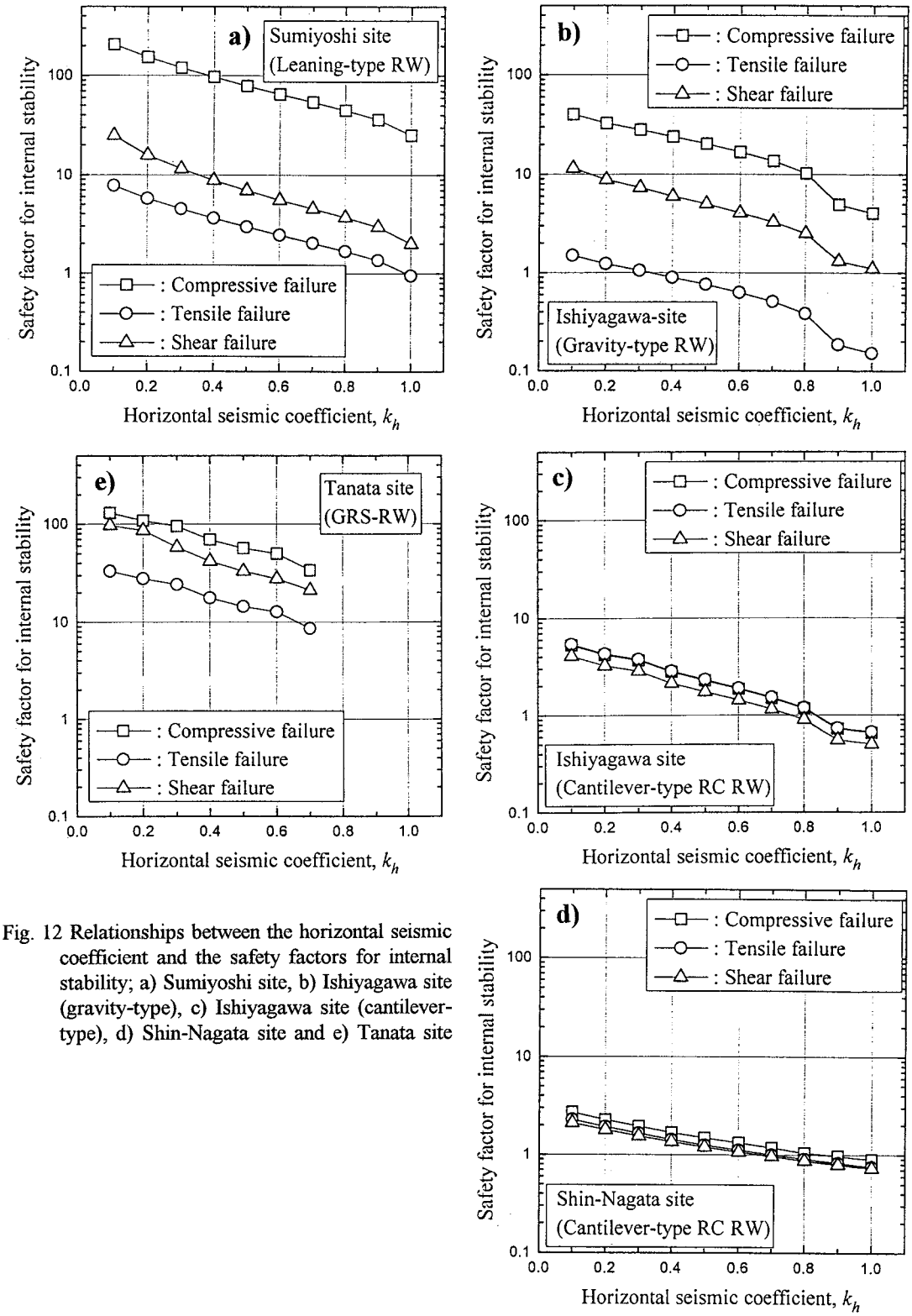

Fig. 12 Relationships between the horizontal seismic coefficient and the safety factors for internal stability; a) Sumiyoshi site, b) Ishiyagawa site (gravity-type), c) Ishiyagawa site (cantilever-type), d) Shin-Nagata site and e) Tanata site

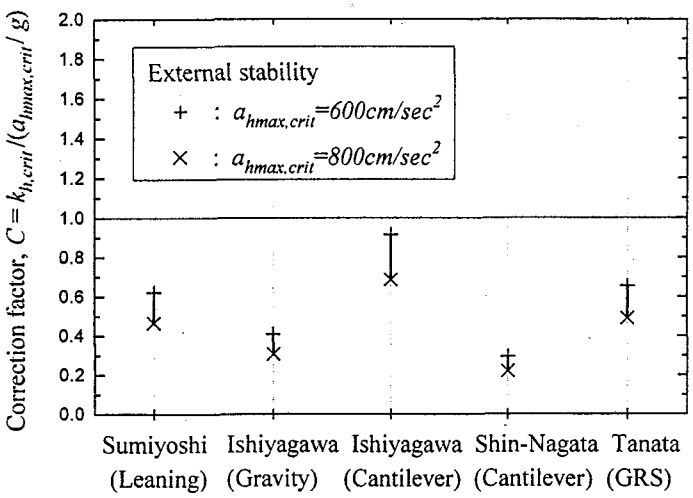

Fig. 13 Correction factor for external stability

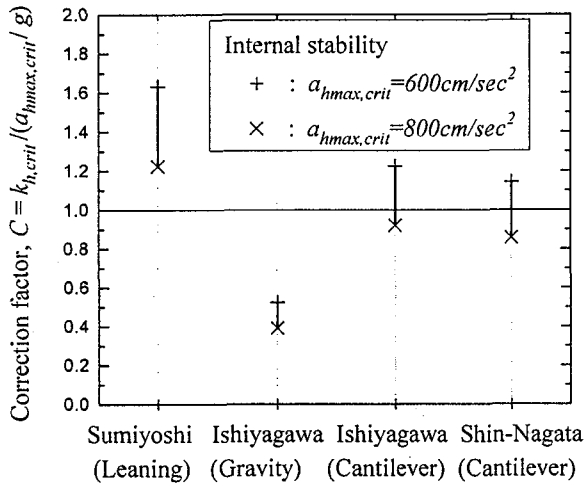

Fig. 14 Correction factor for internal stability